Materials Research. 2023; 26:e20230270
DOI: https://doi.org/10.1590/1980-5373-MR-2023-0270

Rheological Behavior of Alumina Suspensions for Additive Manufacturing Using Digital Light Processing

P.L.A Alves[a]; J.R. Verza[b]; A.P. Luz[a,b]*

[a]*Universidade Federal de São Carlos, Departamento de Engenharia de Materiais, São Carlos, SP, Brasil.*
[b]*Universidade Federal de São Carlos, Programa de Pós-Graduação em Ciência e Engenharia de Materiais, São Carlos, SP, Brasil.*

Received: June 10, 2023; Revised: August 10, 2023; Accepted: September 12, 2023

Additive manufacturing using vat photopolymerization has gained attention for creating intricate ceramic parts. Digital light processing (DLP) is known for its high resolution and speed, but achieving stable ceramic suspensions with high solids concentration and low viscosity is challenging. This study investigated the impact of different dispersants on the rheology and stability of photopolymerizable suspensions. A commercially available water-washable resin, along with three dispersants (Castament FS 10, Triton-X, and DISPERBYK-111), and reactive alumina powder were used to formulate various ceramic suspensions. Viscosity and stability measurements determined the most efficient dispersant and concentration for DLP ceramic part production. Results showed that suspensions with DISPERBYK-111 had optimal viscosity and stability. However, the commercial resin presented higher viscosity, limiting solid loading to 40 vol.% alumina. Successful printing trials were conducted using a commercial printer. The alumina parts were thermally treated at 1550ºC, resulting in ceramics with a good surface finish, well-defined and adhered printed layers, 53.3% relative density, 19.65% XY shrinkage, and 13.69% Z-axis shrinkage.

Keywords: *Viscosity; Alumina; Digital Light Processing; Additive manufacturing; 3D printing.*

1. Introduction

The development of ceramics with complex geometries poses a challenge for traditional processing methods, as they often struggle to achieve the desired geometries and high-quality surface finishes[1,2]. However, new methods have emerged to address these limitations, and among them, additive manufacturing using vat photopolymerization has shown great promise[3]. These manufacturing techniques, commonly employed in the processing of polymeric materials, have recently been explored for producing ceramics with intricate designs[4,5]. Vat photopolymerization encompasses two main methods: Stereolithography (SLA) and Digital Light Processing (DLP). The latter, in particular, stands out for its ability to produce ceramics with exceptional surface finishes, diverse geometries, and rapid processing times[6,7]. In DLP, the printing process occurs layer by layer through the exposure of a photosensitive resin to ultraviolet (UV) light[7].

The successful application of vat photopolymerization in creating ceramic parts heavily relies on the preparation of a stable suspension (comprising a photosensitive resin, ceramic powder, and other additives) with the appropriate rheological properties. Ceramic components fabricated using DLP technology find diverse applications, spanning from essential dental components to cutting-edge uses in space and aerospace engineering, such as in the creation of intricate isogrid structures. Moreover, these meticulously crafted ceramics can also serve as captivating decorative pieces, showcasing both functionality and aesthetic appeal.

During the processing stage, the resin undergoes photo-activation, initiating a radical polymerization reaction that solidifies the regions exposed to light[8]. Various studies recommend the use of suspensions with high solids concentration (at least 40 vol.%) and viscosity below 3 Pa.s to enable the fabrication of dense parts with minimal defects, delamination, or cracks[5,9-15].

In this context, the careful selection of resin type, dispersant additive, and its optimal concentration during suspension preparation plays a crucial role in ensuring the production of high-quality printed parts. Challenges such as increased viscosity and sedimentation of ceramic powders within a short period can significantly compromise the manufacturing process and the properties of the final parts[10-12]. Therefore, this study aims to analyze the influence of different dispersants on the rheological characteristics of ceramic suspensions. Furthermore, based on the best experimental condition obtained, a selected suspension was used to 3D print ceramic parts with complex designs, and their properties were evaluated after thermal treatment at 1550 °C.

2. Experimental Procedure

For the preparation of ceramic suspensions, a reactive alumina powder (A1000SG, d_{50} = 0.52 µm, Almatis, Brazil), a commercial water-washable photosensitive resin (1.10 g/cm^3, 3DLab, Brazil), and three dispersants were used: two types of polyethylene glycol - Castament FS10 (BASF, Germany) and Triton X-100 (Neon, Brazil), and a copolymer DISPERBYK-111 (BYK-111, BYK Chemie).

*e-mail: analuz@ufscar.br

Preliminary tests indicated that the chosen resin showed similar functional groups (carbonyl and C=C[16]) to polyethylene glycol diacrylate (PEGDA, Mn 250, Sigma Aldrich, USA)[9]. Furthermore, this water-washable polymer displayed Newtonian flow behavior (with shear stress increasing linearly with shear rate), and consistent viscosity (~500 mPa.s) across a range of applied shear rate (from 4 to 34 s^{-1}).

Suspensions with 30 or 40% volume fraction of alumina were prepared by mixing the resin, reactive alumina, and dispersants (named here as FS10, Triton, BYK-111) for 24 hours in a ball mill to remove agglomerates and homogenize the mixture, following the procedure suggested in previous studies[12,13]. The prepared mixtures contained different concentrations of dispersant (0, 0.5, 1.0, 2.5, and 5.0 wt.%) calculated based on the initial amount of alumina. After homogenization, the apparent viscosity of these suspensions was evaluated as a function of shear rate and dispersant content using a rotational viscometer (DVT-II Pro, Brookfield, Canada), and the measurements were conducted at room temperature (~25 °C). A total of 5 experiments were carried out for every evaluated composition. In the flow curves, the rheological parameters were adjusted according to the Herschel-Bulkley model[17]:

$$\tau = \tau_e + K\dot{\gamma}^n \quad (1)$$

where τ is the shear stress, τ_e is the yield stress, K is a constant, $\dot{\gamma}$ is the shear rate, and n is the power index. Additionally, the stability of the prepared suspensions was analyzed over 30 days using graduated Falcon tubes to monitor and quantify the sedimentation of alumina particles.

Ceramic specimens were manufactured using a low-cost commercial bottom-up DLP printer (LD-006, Creality, China) with a layer thickness of 50 µm and an exposure time of 1.5 seconds. After printing, the samples were washed with water.

Subsequently, the samples underwent debinding and sintering in a laboratory electric furnace within an ambient air atmosphere to consolidate and densify the resulting microstructure. Table 1 shows the thermal treatment cycle protocol used in this study. The sintered samples were characterized through the following measurements: (i) apparent porosity, water absorption and apparent density according to ASTM C380-00, using water as the immersion liquid; (ii) linear dimensional variation (shrinkage) evaluated in the XY and Z directions of printing, comparing the initial dimensions before debinding process with the final dimensions after sintering step; (iii) relative density of the samples, considering the initial density of alumina as 3.98 g/cm^3.

The resulting microstructure of the printed samples (layer thickness and grain morphology) were evaluated using scanning electron microscopy (Magellan 400 L, FEI, USA). The samples used in these tests were previously polished and thermally etched at 1250 °C for 10 min.

3. Results and Discussion

Figure 1 illustrates the rheological behavior of slurries containing different dispersants at varying concentrations. The dispersant BYK-111 demonstrated the highest effectiveness in reducing the viscosity of the suspension, yielding the best results as its concentration increased up to 5.0 wt.% (Figure 1a). Other researchers have also confirmed the positive impact of this additive on the dispersion of ceramic particles in an organic medium[9]. Dispersant molecules are known to have two types of segments: hydrophilic and hydrophobic. In a non-aqueous medium, it is expected that the hydrophilic segment adsorbs onto the surface of ceramic particles, while the hydrophobic segment forms a steric barrier that prevents other particles from approaching[13,15]. Therefore, it is likely that BYK-111 enabled a greater number of hydrophilic segments to be adsorbed onto the surface of the alumina powder[18], resulting in suspensions with lower viscosity values (Figure 1a).

The suspensions containing Triton X-100 or FS10 exhibited viscosities above 3 Pa·s under the analyzed conditions (Figure 1c and 1e), making these compositions unsuitable for manufacturing ceramic parts via DLP[9,10]. To ensure a fair comparison among the tested slurries, it was decided to use a single type of spindle (SC4-34) for collecting the experimental data. However, some suspensions were highly viscous and could not be analyzed as their viscosity exceeded the measuring range of the rotational viscometer. Triton X-100 was found to be ineffective in the preparation of the tested compositions, as well as in other resin-based systems reported in the literature[9,19]. In fact, the mixtures containing 0.5 or 1.0 wt.% of Triton exhibited even higher viscosities than the reference suspension (0 wt.% or additive-free, Figure 1c).

DISPERBYK 111 showed a near-Newtonian behavior (Figure 1a), whereas the other dispersants demonstrated shear-thinning performance (decreasing viscosity with an increase in shear rate, Figure 1c and 1e). This feature is highly desirable for photocurable suspensions as it prevents particle sedimentation and promotes their flow during the movement of the printing platform[12,20,21]. The stability of the prepared mixtures was assessed by observing the separation of the solid phase (alumina particles) and the liquid phase (resin) after allowing these suspensions to rest for 30 days in 15 mL Falcon tubes. The compositions containing 40 vol.% of alumina exhibited minimal sedimentation with a retained volume fraction of 96.4%.

Table 1. Thermal treatments used in the processing of the printed ceramic samples.

Thermal treatments	Temperature [°C]	Heating rate [°C/min]	Holding time [min]
Debinding	30 – 150	0.5	60
	150 – 400	0.5	15
	400 – 450	0.2	60
	450 – 600	0.5	60
	600 – 1000	5.0	15
Sintering	1550	5.0	60

The flow curves displayed in Figure 1b, 1d and 1f were fitted to the Herschel-Bulkey model[17]. The calculated coefficient of determination (R^2) for all suspensions was higher than 0.999, except for those containing 0.5, 1.0 or 2.5 of Triton X-100 ($R^2 < 0.91$). Table 2 presents the obtained yield stress of the slurries containing different dispersants. However, for certain formulations, this parameter could not be ascertained due to the limited applicability of the Herschel-Bulkley model for fitting. BYK-111 exhibited a low yield stress, particularly when increasing the content of this additive, while the other dispersants showed values ranging from 11.84 to 19.85 Pa. High yield stress is usually considered an obstacle to the spreading of new layers, and this parameter tends to increase with the solid loading[11,22,23].

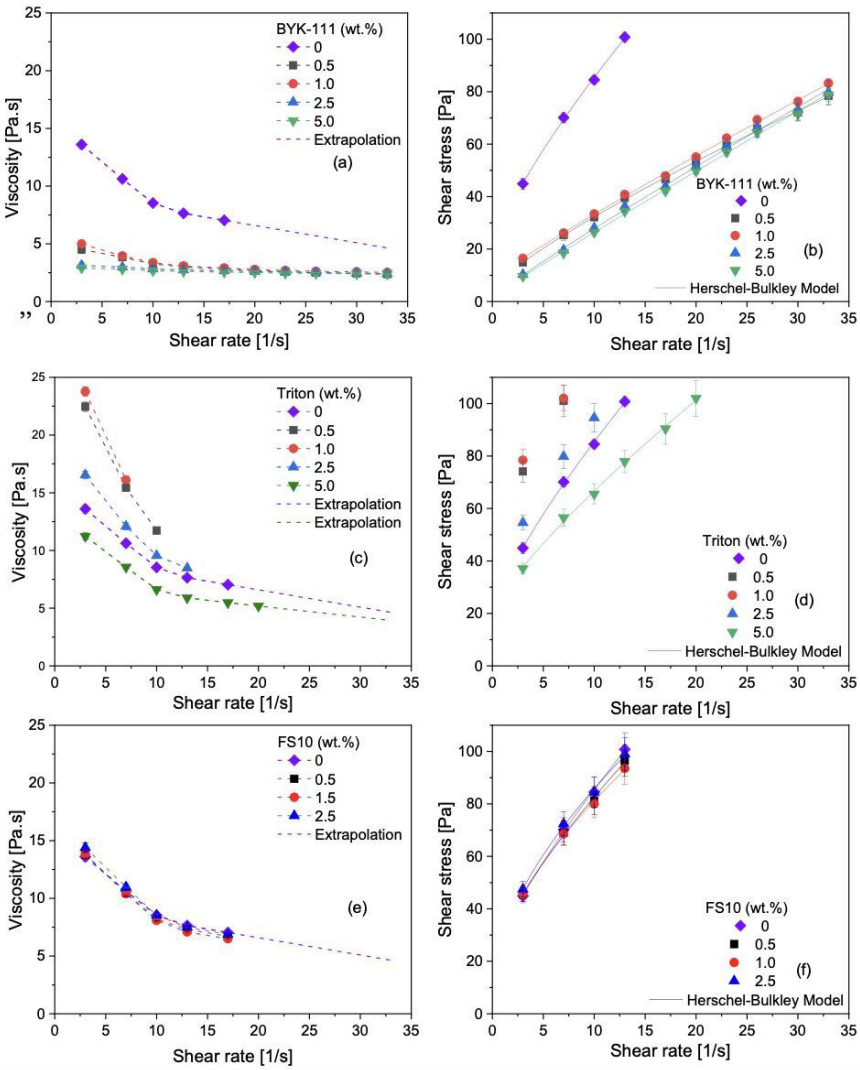

Figure 1. Rheological behavior of ceramic slurries with 40 vol.% solid loading and containing different amounts of the dispersants BYK-111, Triton and FS10. (a, c and e) Viscosity curves as a function of shear rate and (b, d and f) shear stress versus shear rate fitted by the Herschel-Bulkley model.

Table 2. Calculated yield stress values for the slurries containing different concentrations of the selected dispersants.

Dispersant content (wt.%)	Yield stress (Pa)		
	FS10	Triton	BYK-111
0.5	19.85	n.d.	4.61
1.0	13.66	n.d.	8.13
2.5	11.84	n.d.	1.52
5.0	n.d.	19.19	1.83

n.d. = not determined.

Based on the presented results, the dispersant BYK-111 was selected for further tests in this study.

Preliminary printing tests indicated that the suspension containing 40 vol% of alumina and 2.5 wt.% of BYK-111 led to the production of ceramic parts with low quality and surface defects. As a result, additional suspensions with a lower solid loading (30 vol%) were prepared to ensure proper fabrication of the parts.

Figure 2 presents a comparison of the rheological characteristics of ceramic slurries with 30 and 40 vol% solid loading. In Figure 2a, it can be observed that the composition with the lowest measured viscosity (1.48 Pa·s) at a shear rate of 30 s^{-1} (a condition like the one found in DLP printing[10,23]) was achieved by reducing the solid loading to 30 vol% and using 2.5 wt.% of BYK-111. Furthermore, the effect of varying the solid loading on the shear stress of the ceramic suspensions is depicted in Figure 2b. According to the Herschel-Bulkley model, the suspensions exhibited yield stress values close to zero ($R^2 > 0.999$). Moreover, sedimentation tests confirmed the stability of the evaluated formulations containing 30 vol% of alumina particles, as they retained 96.5% of the original volume. This behavior was considered suitable for the printing process and indicated the need for further experimentation.

Complex geometry parts were produced using the developed suspension containing 30 vol% solids and 2.5 wt.% of BYK-111. In general, the samples showed good reproduction of the details in the chosen design (Figure 3). However, some surface irregularities were observed, despite using a low viscosity suspension (1.48 Pa.s) for the printing process. This may be attributed to the use of a commercial printer originally designed for processing pure polymeric suspensions without ceramic particles. Additionally, the presence of oxide particles in the suspension can scatter ultraviolet light, affecting the resin's photopolymerization process and potentially leading to shape inaccuracies in the printed parts.

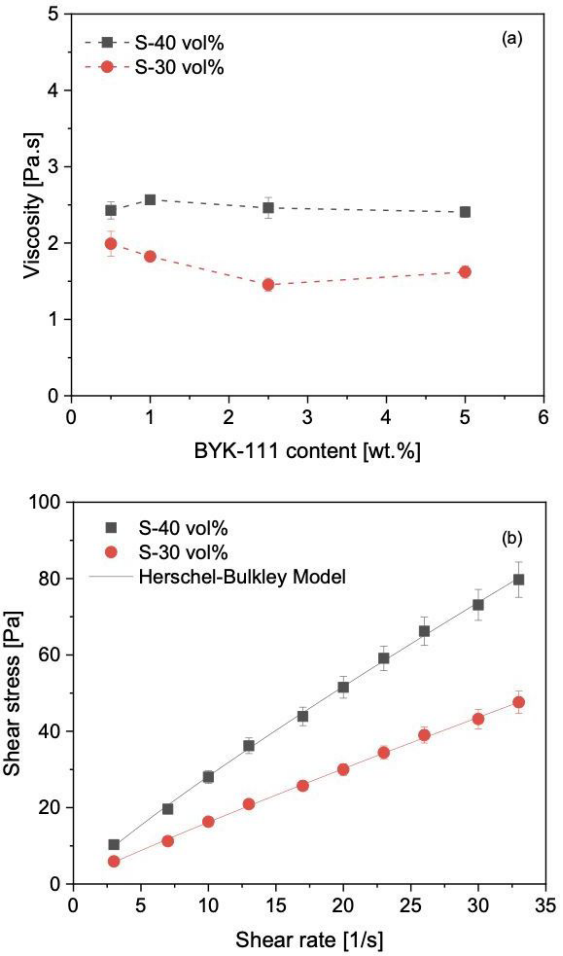

Figure 2. Comparison of the rheological behavior of ceramic slurries with 30 and 40 vol% solid loading: (a) viscosity profiles of slurries with different concentrations of BYK-111 at a shear rate of 30 s^{-1}; (b) shear stress versus shear rate curves fitted using the Herschel-Bulkley model.

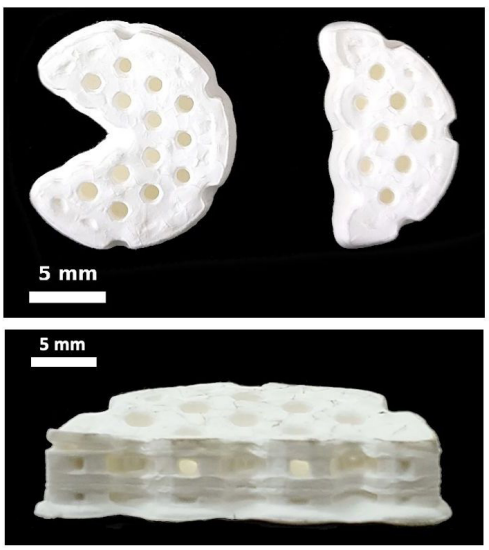

Figure 3. Images of the alumina parts obtained using the digital light processing (DLP) technique.

Table 3. Characterization of the sintered* ceramic parts manufactured via DLP technique.

XY Shrinkage [%]	Z Shrinkage [%]	Apparent porosity [%]	Water absorption [%]	Relative density [%]
19.6 ± 0.5	13.7 ± 1.5	23.2 ± 0.5	10.9 ± 0.3	53.3 ± 0.6

*Sintering step at 1550°C for 1 hour.

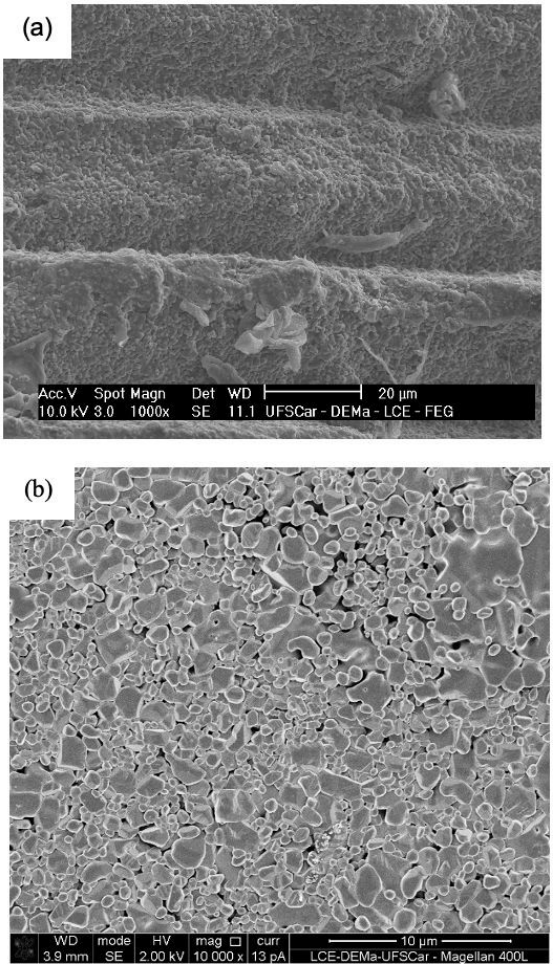

Figure 4. SEM images of the ceramic samples produced using DLP technique and sintered at 1550°C for 1 hour. (a) Detail of the printed layers, and (b) distribution of alumina grains in the resulting microstructure.

The fabricated samples underwent heat treatments to remove the resin and densify the microstructure. After firing at 1550 °C for 1 hour, parts with a relative density of 53.3%, linear shrinkage of 19.6% in the XY direction, and 13.7% in the Z direction were obtained (Table 3). It is worth noting that in other studies, the linear shrinkage of the prepared ceramic specimens was typically higher in the Z-axis[24,25]. However, the presented data deviate from this trend due to the low concentration of solids (30 vol%) used in the initial suspension. This low solid concentration also limited the densification of the produced parts as a significant amount of organic matter was removed during the debinding step. Consequently, the samples exhibited an apparent porosity of 23.2% and water absorption of 10.9% after firing.

The microstructure of the sintered samples was analyzed using scanning electron microscopy (SEM). Figure 4 illustrates that the layers formed during the printing process displayed excellent bonding and adhesion, resulting in an average layer thickness of 31.07 ± 0.67 µm. The actual layer thickness was typically smaller than the initially programmed value due to the scattering of ultraviolet light by the solid components of the suspension. Furthermore, the microstructure exhibited uniform distribution of pores and alumina with a median grain size of 1.09 µm.

4. Final Remarks

Three dispersants (Castament FS10, Triton-X, and DISPERBYK-111) were tested at different concentrations during the preparation of suspensions comprising a water-washable commercial resin and containing 30 or 40 vol.% of alumina particles for processing and manufacturing ceramic parts using the DLP technique. Among the tested dispersants, BYK-111 demonstrated superior effectiveness in dispersing the ceramic powder in the organic medium, leading to compositions with lower viscosity (up to 2.5 Pa·s). However, even with the improved dispersion, the suspensions containing 40 vol% of solids still demonstrated unsuitability for the printing process using a commercial printer.

Optimal printing conditions were achieved by preparing a suspension consisting of 30 vol% alumina and 2.5 wt.% of the dispersant BYK-111. This formulation exhibited a viscosity of 1.48 Pa.s at room temperature and demonstrated adequate stability with a volume retention of 96.5% even after 30 days. Nevertheless, owing to the limited solid content of the examined suspensions (30 vol%), the resultant components attained a relative density of only 53.3 ± 0.6%. The printed parts displayed well-adhered layers with excellent bonding after sintering at 1550°C for 1 hour. Despite the identified limitations, the use of a commercial printer not specifically designed for ceramics proved to be an attractive and cost-effective solution for producing small ceramic parts with complex geometries.

5. Acknowledgments

This study was financed in part by the Coordenação de Aperfeiçoamento de Pessoal de Nível Superior - Brasil (CAPES) - Finance Code 001. This work was carried out with the support of CNPq, Conselho Nacional de Desenvolvimento Científico e Tecnológico - Brazil, and Coordenadoria dos Programas de Iniciação Científica e Tecnológica (CoPICT - UFSCar). The authors would also like to thank Almatis and BYK for supplying the raw materials used in this work.

6. References

1. Zhang K, Xie C, Wang G, He R, Ding G, Wang M, et al. High solid loading, low viscosity photosensitive Al_2O_3 slurry for stereolithography based additive manufacturing. Ceram Int. 2019;45(1):203-8. http://dx.doi.org/10.1016/j.ceramint.2018.09.152.
2. Zakeri S, Vippola M, Levänen E. A comprehensive review of the photopolymerization of ceramic resins used in stereolithography. Addit Manuf. 2020;35:101177. http://dx.doi.org/10.1016/j.addma.2020.101177.
3. Tian C, Wu J-M, Wu Y-R, Liu C-L, Lin X, Shi Y-S. Effect of polystyrene addition on properties of porous Si3N4 ceramics fabricated by digital light processing. Ceram Int. 2023;49(16):27040-9. http://dx.doi.org/10.1016/j.ceramint.2023.05.246.
4. Zhou M, Liu W, Wu H, Song X, Chen Y, Cheng L, et al. Preparation of a defect-free alumina cutting tool via additive manufacturing based on stereolithography: optimization of the drying and debinding processes. Ceram Int. 2016;42(10):11598-602. http://dx.doi.org/10.1016/j.ceramint.2016.04.050.
5. Truxova V, Safka J, Seidl M, Kovalenko I, Volesky L, Ackermann M. Ceramic 3D printing: comparison of SLA and DLP technologies. MM Sci J. 2020;2020(2):3905-11. http://dx.doi.org/10.17973/MMSJ.2020_06_2020006.
6. Wang D, Chen T, Zeng Y, Chen X, Xing W, Fan Y, et al. Optimization of UV-curable alumina suspension for digital light processing of ceramic membranes. J Membr Sci. 2022;643:120066. http://dx.doi.org/10.1016/j.memsci.2021.120066.
7. Abdulhameed O, Al-Ahmari A, Ameen W, Mian SH. Additive manufacturing: challenges, trends, and applications. Adv Mech Eng. 2019;11(2):1-27. http://dx.doi.org/10.1177/1687814018822880.
8. Zhang J, Yu KB, Wu JM, Ye CS, Zheng W, Liu H, et al. Effects of ZrSiO4 content on properties of SiO2-based ceramics prepared by digital light processing. Ceram Int. 2023;49(6):9584-91. http://dx.doi.org/10.1016/j.ceramint.2022.11.128.
9. Camargo IL, Erbereli R, Taylor H, Fortulan CA. 3Y-TZP DLP additive manufacturing: solvent-free slurry development and characterization. Mater Res. 2021;24(2):e20200457. http://dx.doi.org/10.1590/1980-5373-mr-2020-0457.
10. Camargo IL, Morais MM, Fortulan CA, Branciforti MC. A review on the rheological behavior and formulations of ceramic suspensions for vat photopolymerization. Ceram Int. 2021;47(9):11906-21. http://dx.doi.org/10.1016/j.ceramint.2021.01.031.
11. Mu Y, Chen J, An X, Liang J, Li J, Zhou Y, et al. Defect control in digital light processing of high-solid-loading ceramic core. Ceram Int. 2022;48(19):28739-44. http://dx.doi.org/10.1016/j.ceramint.2022.06.141.
12. Wozniak M, de Hazan Y, Graule T, Kata D. Rheology of UV curable colloidal silica dispersions for rapid prototyping applications. J Eur Ceram Soc. 2011;31(13):2221-9. http://dx.doi.org/10.1016/j.jeurceramsoc.2011.05.004.
13. Adake CV, Bhargava P, Gandhi P. Effect of surfactant on dispersion of alumina in photopolymerizable monomers and their UV curing behavior for microstereolithography. Ceram Int. 2015;41(4):5301-8. http://dx.doi.org/10.1016/j.ceramint.2014.12.066.
14. Sun J, Binner J, Bai J. Effect of surface treatment on the dispersion of nano zirconia particles in non-aqueous suspensions for stereolithography. J Eur Ceram Soc. 2019;39(4):1660-7. http://dx.doi.org/10.1016/j.jeurceramsoc.2018.10.024.
15. Zhang S, Sha N, Zhao Z. Surface modification of α-Al2O3 with dicarboxylic acids for the preparation of UV-curable ceramic suspensions. J Eur Ceram Soc. 2017;37(4):1607-16. http://dx.doi.org/10.1016/j.jeurceramsoc.2016.12.013.
16. Imani M, Sharifi S, Mirzadeh H, Ziaee F. Monitoring of polyethylene glycoldiacrylate-based hydrogel formation by real time NMR spectroscopy. Iran Polym J. 2007;16:13-20.
17. Herschel WH, Bulkley R. Konsistenzmessungen von gummibenzollosungen. Colloid Polym Sci. 1926;39(4):291-300. http://dx.doi.org/10.1007/BF01432034.
18. Xing Z, Zhou H, Liu W, Nie J, Chen Y, Li W. Efficient cleaning of ceramic green bodies with complex architectures fabricated by stereolithography-based additive manufacturing via high viscoelastic paste. Addit Manuf. 2022;55:102809. http://dx.doi.org/10.1016/j.addma.2022.102809.
19. Wu Z, Liu W, Wu H, Huang R, He R, Jiang Q, et al. Research into the mechanical properties, sintering mechanism and microstructure evolution of Al2O3-ZrO2 composites fabricated by a stereolithography-based 3D printing method. Mater Chem Phys. 2018;207:1-10. http://dx.doi.org/10.1016/j.matchemphys.2017.12.021.
20. Dufaud O, Marchal P, Corbel S. Rheological properties of PZT suspensions for stereolithography. J Eur Ceram Soc. 2002;22(13):2081-92. http://dx.doi.org/10.1016/S0955-2219(02)00036-5.
21. Sokolov PS, Komissarenko DA, Dosovitskii GA, Shmeleva IA, Slyusar' IV, Dosovitskii AE. Rheological properties of zirconium oxide suspensions in acrylate monomers for use in 3D printing. Glass Ceram. 2018;75(1-2):55-9. http://dx.doi.org/10.1007/s10717-018-0028-3.
22. Zhang K, He R, Xie C, Wang G, Ding G, Wang M, et al. Photosensitive ZrO_2 suspensions for stereolithography. Ceram Int. 2019;45(9):12189-95. http://dx.doi.org/10.1016/j.ceramint.2019.03.123.
23. Xing B, Cao C, Zhao W, Shen M, Wang C, Zhao Z. Dense 8 mol% yttria-stabilized zirconia electrolyte by DLP stereolithography. J Eur Ceram Soc. 2020;40(4):1418-23. http://dx.doi.org/10.1016/j.jeurceramsoc.2019.09.045.
24. Liu CL, Du Q, Zhang C, Wu JM, Zhang G, Shi YS. Fabrication and properties of BaTiO3 ceramics via digital light processing for piezoelectric energy harvesters. Addit Manuf. 2022;56:102940. http://dx.doi.org/10.1016/j.addma.2022.102940.
25. Liu CL, Lu L, Wu JM, Wang CA, Shi YS. Preparation and properties of $0.79ZnAl_2O_4$-$0.21TiO_2$ microwave dielectric ceramics via digital light processing. J Alloys Compd. 2022;911:165095. http://dx.doi.org/10.1016/j.jallcom.2022.165095.